Submitted to: Progress In Computational Fluid Dynamics: An International Journal

Second-Order Conditional Moment Closure Modelling of H_2/He Turbulent Jet Diffusion Flames

M. Fairweather and R.M. Woolley

School of Process, Environmental and Materials Engineering
The University of Leeds
Leeds LS2 9JT
United Kingdom

Corresponding Author for Review Process: Prof. M. Fairweather,
Department of Chemical Engineering,
School of Process, Environmental
and Materials Engineering,
University of Leeds,
Leeds LS2 9JT,
UK.
Telephone: +44 (0) 113 343 2419
Facsimile: +44 (0) 113 343 2405
E-mail: m.fairweather@leeds.ac.uk

Abstract - The advent of increasingly stringent emissions legislation inevitably leads to the requirement for more accurate modelling of pollutant formation in practical combustion applications. Previous limited success in modelling species such as NO using first-order conditional moment closure (CMC) models indicates the need for more advanced modelling techniques. Here, a method of including higher-order chemistry within a one-dimensional, parabolic CMC framework is investigated, and applied to the prediction of three hydrogen jets of varying degrees of helium dilution. Interaction of the combustion model with both the k-ε and Reynolds stress turbulence models is examined. Results are encouraging, and found to be in line with expectations. Suggestions are made in light of this to account for anomalous predictions of nitrous radical formation.

Keywords: Conditional moment closure, first-/second-order, turbulent flames, hydrogen/ helium, emissions

Biographical Notes

Eur Ing **Dr. M. Fairweather** *BSc, PhD, CEng, MEI, MIChemE, MIMechE, CPhys, MInstP* is a Reader within the School of Process, Environmental and Materials Engineering at the University of Leeds. He joined the University in 1998 having worked for British Gas for the previous seventeen years. Dr. Fairweather has been engaged in research in the areas of fluid dynamics, chemical kinetics and combustion, heat transfer and thermodynamics for more than twenty years, with his primary interest being the development and application of computational fluid dynamic techniques. He has extensive experience of developing and using CFD codes in gas utilisation applications (including gas turbines, furnaces, boilers and re-burn systems), as well as in safety and environmental applications, and has developed basic mathematical descriptions of turbulent and combusting flows in addition to models of convection and radiation heat transfer. Dr. Fairweather has contributed more than seventy papers to the technical literature.

Dr. R.M. Woolley *BEng, PhD, AMIChemE* is a Research Officer within the School of Process, Environmental and Materials Engineering at the University of Leeds, and joined the Department of Chemical Engineering after completing his post-graduate research at the University in 2002. His doctoral thesis encompassed aspects of combustion modelling, incorporating studies of chemical kinetics, thermodynamics and fluid dynamics, implemented via the development of computational fluid dynamic codes. Currently he is involved with the development of novel mathematical descriptions of turbulent reacting flows, and their application to combustion emissions from confined gas flames as found in industrial boilers and turbines, amongst many applications. Dr. Woolley has made recent contributions to the technical aspects of the field by means of publications in relevant peer-reviewed journals and by presentation at international conferences.

1. Introduction

Central to the design and analysis of practical combustion devices is the prediction of scalar and vector quantities in turbulent reacting flows. In recent years, the desire for efficiency improvement and emissions reduction in combustion reactions has highlighted the need to link turbulent flow and finite-rate chemistry calculations in the modelling of such flows.

A number of differing approaches have been proffered as a solution to the representation of the interactions of turbulent fluctuations and density changes effected by chemical reaction. To date, the two most promising are the transported probability density function (PDF) [1] and the conditional moment closure (CMC) [2] methodologies. The PDF approach includes the effects of finite-rate chemistry via the solution of the multi-dimensional PDF of scalar, and in some cases vector, quantities. The nature of this problem leads to a Monte Carlo solution procedure being adopted, requiring significant computing resources. This can prove to be a limiting factor in the physical dimensionality of the problems that can be addressed in practical applications. The CMC method on the other hand provides a more computationally economical method by which kinetic effects can be included in calculations. This enables the study of more complex geometries, and the consideration of a greater number of scalar variables for a given problem. Essentially, the greatest obstacle in such calculations is the problem associated with a high degree of non-linearity of the reaction-rate terms within the species transport equations. The CMC approach eliminates this non-linearity by the consideration of various moments of species concentrations, conditionally averaged at a fixed value of a conserved scalar variable, and the assumption that fluctuations in these scalar values are negligible about their mean in the conditional dimension. In the application to non-premixed combustion, the conditioning variable is typically taken to be the mixture fraction, and the overall method is described as n^{th} order, dependant upon the order of conditional

moments evaluated within the CMC transport equation. The focus of the present work is an assessment of first- and second-order CMC methods, and a comparison of their performance.

CMC has been successfully applied to a number of practical situations such as premixed and non-premixed combustion, and ignition and extinction phenomena. The majority of works to date have applied first-order parabolic models to simple flows such as hydrogen [3-5], methanol [6], CO/CO_2 [7, 8] and methane [9, 10] diffusion flames. Elliptic methods have also been applied to more complex geometries such as bluff-body stabilised flows as described in [11, 12], and to the prediction of lifted jet flames [13]. Previous limited success in modelling NO formation in a number of these flames using the first-order approach indicates the possible need to consider second- or higher-order effects of chemistry upon the species production rates. Temperature, and hence density fluctuations, can have notable effects upon these variables, with NO thermal production pathways being particularly sensitive to such variations. Kronenburg et al. [14] confirm this surmise in their calculations of helium-diluted hydrogen jets using a higher-order closure technique.

The application of second-order CMC methods to jet diffusion flames has, to date, not been extensively investigated. However, recently, Bradley et al. [15] purport generally good results for major species predictions in their application of a flamelet model/CMC hybrid, but fail to obtain a similar level of agreement for the prediction of intermediate species. Seminal work concerning the higher-order modelling of autoignition was executed by Mastorakos and Bilger [16], and Kim et al. [17] develop a higher-order closure for hydrocarbon fuels, applying this to modelling of the extinction and reignition phenomena of a direct numerical simulation of such flames with some success. They also note an improvement in predictions of primarily intermediate species over the first-order model, and extend their studies to include piloted methane jets [18], again noting agreeable results conforming to theoretical expectations.

Presented in this paper are the results from first- and second-order CMC calculations of the H_2/He diffusion flames of Barlow and Carter [19]. The study of hydrogen combustion is a useful tool in the analysis of modelling techniques because of the relative simplicity of the chemistry involved. The study of NO production is facilitated by the exclusion of the fuel- and prompt-NO production mechanisms, and the absence of sooting which influences the flame temperature via radiation. The addition of helium provides additional test-cases to work with, but also acts to further reduce the radiant fraction to very low levels in these flames. In light of previous works by the authors involving these [5] and other [10] flames, all calculations are carried out within a Reynolds stress/turbulent scalar flux turbulence modelling framework. However, the only other investigation of second-order effects within these flames [14] has been carried out with k-ε closure calculations, and hence comparisons are made between the effects of these two turbulence closures on second-order CMC calculations.

2. Mathematical Model

The combusting flows investigated in this paper are the three well documented H_2/He turbulent jet diffusion flames as reported by Barlow and Carter [19], consisting of hydrogen with 0, 20 and 40 percent helium dilution, being subsequently referred to as Flames A, B and C. Centred at the exit of a wind tunnel, the flames are unpiloted, and issue from a 3.75 mm diameter nozzle at respective axial velocities of 296, 294 and 256 m s^{-1} into a co-flowing air stream of velocity 1 m s^{-1}. Further details regarding the flow parameters and experimental rig can be found in the above-mentioned reference.

2.1 Turbulent Flow Calculations

The flow and mixing fields were resolved by the solution of the two-dimensional, axisymmetric forms of the density-weighted fluid flow equations, supplemented with the k-ε model in one instance, and with a Reynolds stress/scalar flux closure in the second. Closure of the mean density term was achieved using a prescribed β-PDF, with instantaneous values of density, as a function of mixture fraction, derived from adiabatic equilibrium calculations based on the twelve species, twenty-six step reaction scheme employed and validated in previous works [3, 5]. Standard constants [20] were employed in the k-ε model, and the Reynolds stress/scalar flux model [21], with only minor and accepted modifications being made to the $C_{\varepsilon 1}$ constant to improve the spreading rate predictions. The requirement for these modifications is expected as they fall in line with the 'round-/plane-jet anomaly'. As observed by el-Baz et al. [22], parabolized 'boundary-layer' calculations produce results significantly different to those obtained from Navier-Stokes calculations, due in part to the effects of longitudinal stress gradients and the longitudinal diffusion of the dissipation rate.

Solution of the transport equations was achieved using a modified version of the GENMIX code [23]. This uses a time-marching approach to simulate the parabolic flow field of interest, and employs a coordinate transformation method with a normalised stream function for the efficient solution of the equations over a grid restricted to the width of the boundary layer. Numerical solutions were obtained using expanding finite-difference meshes, and in all cases, grid independent solutions were established using resolutions in excess of one million nodes. Inlet boundary conditions were prescribed from experimental data, and where not available were defined using turbulence theory [24]. Hence, turbulence energy and its dissipation were represented at the pipe exit as Equations (1) and (2) respectively.

$$k = 0.0027u^2 \qquad (1)$$

$$\varepsilon = \frac{k^{3/2}}{0.5d} \tag{2}$$

2.2 First-Order, One-Dimensional CMC Model

Averaging the instantaneous equations governing reactive scalar transport and production in statistically stationary, turbulent reacting flows, on the condition that the instantaneous mixture fraction equals an arbitrary value (η), leads to a set of equations describing the production and transport of the conditionally averaged scalars and enthalpy. With reference to simplifying assumptions outlined by Klimenko and Bilger [2], flows of the type in question, displaying properties associated with high Reynolds number and being far from extinction, allow the simplifying assumptions of negligible macro-transport by molecular diffusion and negligible turbulent flux contributions. In addition, such flows display little cross-stream variation in conditional statistics, allowing a reduction in the problem dimensionality, and hence the constituents of the CMC equation are cross-stream averaged as defined by Klimenko [25]. The governing equations for species mass fraction and enthalpy then become, respectively:

$$\frac{\partial Q_i}{\partial x}\langle u \mid \eta \rangle = \frac{1}{2}\langle \chi \mid \eta \rangle \frac{\partial^2 Q_i}{\partial \eta^2} + \langle w_i \mid \eta \rangle \tag{3}$$

$$\frac{\partial Q_h}{\partial x}\langle u \mid \eta \rangle = \frac{1}{2}\langle \chi \mid \eta \rangle \frac{\partial^2 Q_h}{\partial \eta^2} + \langle w_h \mid \eta \rangle, \tag{4}$$

where the angular brackets denote ensemble averaging of the conditional expectation. The conditional average velocity was defined as the PDF-weighted, cross-stream averaged value, and the approach of Girimaji [26] was implemented to describe the conditional scalar dissipation. The non-linear conditional source term is approximated as for first-order closure,

assuming fluctuations of production rate around the mean to be negligible. These mean values were obtained using the CHEMKIN package [27] in conjunction with the kinetics scheme discussed in section 2.1, references 3 and 5, and listed fully as Table 1. The reaction steps are extracted from the mechanism described by Miller and Bowman [28], with the exception of the two body shuffle reactions governing production of the radicals H, O and OH which are drawn from the skeletal mechanism described by Smooke and Giovangigli (29).

2.3 Second-Order, One-Dimensional CMC Model

A full second-order closure of reaction rate terms would require the solution of variance and covariance equations for all species considered. This proves limiting in terms of computational efficiency, and so for the present study a method similar to that employed by Kronenburg et al. [14] is adopted. In the present study, a simplified chemical system of the seven species H_2, O_2, H_2O, O, H, OH, and HO_2 is used to describe the composition at any given value of mixture fraction, enthalpy and of the progress variable Γ, defined as the total number of moles in the system by Equation 5.

$$\Gamma = \sum_{\alpha=1}^{i} \frac{M_\alpha}{W_\alpha} \tag{5}$$

For any given value of mixture fraction and enthalpy, an instantaneous reaction rate is then defined by integrating the product of the distribution and the PDF over Γ space. For this purpose, a β-PDF is assumed, which requires a variance of Γ for its definition. This is established via the solution of one additional scalar transport equation for the conditional variance ($\left\langle \Gamma''^2 \middle| \eta \right\rangle$) of Γ, the derivation of which can be followed in Li and Bilger [28] and is defined in a one-dimensional form by Equation (6). For brevity, a nomenclature has been

$$\frac{\partial G}{\partial t}+\langle u|\eta\rangle\frac{\partial G}{\partial x}-\langle \chi|\eta\rangle\frac{\partial^2 G}{\partial \eta^2}+\frac{\frac{\partial}{\partial x}\left(\langle \rho|\eta\rangle\langle u''K''|\eta\rangle P(\eta)\right)}{P(\eta)\langle \rho|\eta\rangle}= \\ 2\langle w''\Gamma''|\eta\rangle-2\left\langle D\left(\frac{\partial \Gamma''}{\partial x}\right)^2\middle|\eta\right\rangle-2\frac{\partial Q_\Gamma}{\partial x}\langle u''\Gamma''|\eta\rangle+2\frac{\partial^2 Q_\Gamma}{\partial \eta^2}\langle \chi''\Gamma''|\eta\rangle \tag{6}$$

adopted regarding which the reader should refer to the section 5 for a full description. Applying similar assumptions to the first-moment equation and incorporating additional means of closure, the closed form with exception of the conditional reaction-rate correlation term, can be described as Equation (7). Numbering the terms of Equation (6) sequentially from left to right, term 4 has been neglected as the contribution to transport from conditional fluctuations is considered to be negligible in these high Reynolds number flows. The

$$\langle u\,|\,\eta\rangle\frac{\partial G}{\partial x}=\langle \chi\,|\,\eta\rangle\frac{\partial^2 G}{\partial \eta^2}+2\langle w''\Gamma''\,|\,\eta\rangle-1.82\left(\frac{\varepsilon}{k}\right)G+1.1\langle \chi\,|\,\eta\rangle(G)^{1/2}\frac{\partial^2 Q_\Gamma}{\partial \eta^2} \tag{7}$$

generation term, number 7 has also been neglected after considering the transverse gradients of Q to be small in most shear flows. Referring to Li and Bilger (30), the dissipation term number 6 has been modelled using the integral time scale, and their suggestions applied to the representation of term 8, this being generation due to χ fluctuations. The constants 1.82 and 1.1 are justified in the authors' works.

In the modelling of the reaction-rate correlation term, it is assumed that the kinetics system in question can be represented by the single-step global reaction $2H_2+O_2\rightarrow 2H_2O$ (31). The reaction rate of this step (w_Γ) can then be defined in terms of the relatively slow recombination reactions used in the prescription of first-order chemistry, and the correlation term obtained via Equation (8). The superscript 'pe' in this equation refers to the usage of

partial equilibrium assumptions for the evaluation of the reaction rate as subsequently discussed.

$$\begin{aligned}\left\langle w''\Gamma'' \,|\, \eta \right\rangle &= \left\langle w_\Gamma \Gamma \,|\, \eta \right\rangle - \left\langle w_\Gamma \,|\, \eta \right\rangle \left\langle \Gamma \,|\, \eta \right\rangle \\ &\approx \int_\Gamma w_\Gamma^{pe}(\eta,\Gamma)\Gamma P(\eta,\Gamma)d\Gamma - \left\langle \Gamma \,|\, \eta \right\rangle \int_\Gamma w_\Gamma^{pe}(\eta,\Gamma)P(\eta,\Gamma)d\Gamma\end{aligned} \tag{8}$$

Equation (7) is then solved alongside those defined for first-order closure, and corrections to the rates obtained via implementation of Equation (9).

$$\left\langle w_r \,|\, \eta \right\rangle_{2ord} = \left\langle w_r \,|\, \eta \right\rangle + \left\langle w_{r,corr}^{pe} \,|\, \eta \right\rangle . \tag{9}$$

$$\left\langle w_{r,corr}^{pe} \,|\, \eta \right\rangle = \left\langle w_r^{pe} \,|\, \eta \right\rangle - w_r^{pe}\left(\left\langle \Gamma \,|\, \eta \right\rangle, \eta\right) \tag{10}$$

$$\left\langle w_r^{pe} \,|\, \eta \right\rangle = \int_\Gamma w_r^{pe}(\eta,\Gamma)P(\eta,\Gamma)\,d\Gamma \tag{11}$$

The corrections to the first-order rates are obtained via the equality given by Equation (10), with the mean value having been obtained by the integration over Γ-space as shown by Equation (11).

The set of simultaneous equations required for elucidation of the chemical and energetic composition of the system as a function of Γη and enthalpy was derived from balances on the system enthalpy, O atom, H atom and the total number of moles in the system, supplemented with equations for the radicals H, O, and OH, obtained by partial equilibrium assumptions. Assuming steady state for the HO_2 molecule, an expression for its molar concentration was implemented as defined by Montgomery at al. [32]. It may be noted that initially, integration of this system proved to be problematic via a Newton-Raphson technique and, as noted by Kronenburg et al. [14], convergence of solution under certain circumstances

was unobtainable. The aforementioned authors developed another form of calculation to circumvent this problem, namely a Taylor expansion of the sink term in Equation (3). In the present work, however, equation systems of differing variables and definition were investigated. A numerically stable system was eventually prescribed with solution via the Newton-Raphson method, which differed to the work of Kronenburg et al. [14] by the omission of nitrogen and the inclusion of HO_2 to the species solved for in the second-order approach.

3. Results and Discussion

Limitation of space prevents a detailed analysis of the velocity and mixing field predictions obtained from the application of the two turbulence models. However, good agreement was found with the experimental data on H_2/He diffusion flames of Barlow and Carter [19], with the Reynolds stress model displaying generally superior results over the three flames investigated. Figure 1 depicts conditional velocity and scalar dissipation at three axial stations, calculated for Flame A, from the aforementioned data. This figure highlights the discrepancies between the two differing flow field predictions, which can be seen to manifest in the conditional statistics. Similar results were found in the other flames investigated, and go someway to highlighting the importance played by the flow field model specification in calculations such as these. Further discussion regarding these results can be found in Fairweather and Woolley [5], which also provides a more substantial analysis of data obtained using the first-order CMC model.

Figure 2 depicts first- and second-order CMC predictions of major species and temperature in Flame A, obtained in conjunction with a Reynolds stress turbulence closure. It can be seen that at all locations, predictions are in good agreement with data, excepting an under-prediction of temperature at the first measurement station. This is due to an under-prediction

of mixing, observed in the flow field calculations [5]. Differences observed between the two chemistry schemes are minimal, though a slight decrease in temperature and H_2O formation is observed on the rich side of stoichiometric for the higher order case. This is accounted for as effects due to second-order radical depletion as a consequence of recombination reaction enhancement.

Figures 3 and 4 depict OH and NO predictions in composition space, plotted against experimental data at three axial locations for Flames A and B respectively. Both first- and second-order results are shown, having been derived in conjunction with a Reynolds stress turbulence model. With respect to NO predictions, the second-order corrections can be seen to decrease the peak values at all locations, effecting a shift across both fuel-lean and fuel-rich data. The magnitude of this adjusted value, relative to the first-order predictions, is seen to decrease with axial distance in line with the evolution of the conditional variance, which displays its maxima prior to reaching the first measurement station in the region of thirteen nozzle diameters. This trend was also notable for Flame C (not shown) and, in addition, the relative magnitude of the correction was found to increase from Flames A to B, and to C. The resultant of the second-order application can be considered comparable to that observed by Kronenburg et al. [14] in a qualitative sense, excepting data at the first measurement station. The present study shows a greater deviation of second-order results from the experimental data than the respective first-order calculation, whereas Kronenburg et al. [14] show a negligible difference. Comparisons of the first- and higher-order calculations closer to the nozzle (not shown) for the three flames do, however, show similar results in the current work. The same observations can be extended to predictions of the OH radical for all three flames, although the greatest influence of second-order chemistry appears to be on the rich-side of stoichiometric in all cases. With attention drawn to quantitative analysis, the higher-order model is generally not seen to improve NO predictions across the three flames, but does

display an expected trend in results. The correction terms enhance the slower three-body recombination reactions, resulting in lower rates of NO formation at upstream locations. However, in the majority of cases, the first-order predictions can be seen to be of a good level of agreement with experimental data, or indeed display an under-prediction, and hence a second-order correction only acts to worsen estimations. The exception can be seen in Flame B, where at 112.5 nozzle diameters, the second-order prediction is a marked improvement, and falls into agreement with experiment for lean stoichiometries and peak value, although still slightly over-predicting in fuel-rich regions. This however is not the case with respect to OH predictions, which all display a considerable improvement, although relatively minor in magnitude. In the majority of cases, first-order estimations notably over-predict OH peak levels and data on the fuel-rich side of stoichiometric, and the second-order effect upon the recombination reactions can be seen to bring these levels into line with experimental findings; corrections being more evident in the fuel-rich regions.

The effect on rich mixtures is noted in previous works [13, 14], and means of explanation is not proffered until more recent work regarding the modelling of differential diffusion in these flows [33]. With the inclusion of such effects, Kronenburg and Bilger [33] establish the non-unity of the H ion Lewis number is responsible for the super-equilibrium temperatures on the lean side of stoichiometric, and hence improve OH predictions in this region. They also establish an improvement in NO at the near-field measurement station by an increase of around sixty percent of the equal-diffusivity counterparts. Also observed is the negligible effect of differential diffusion on results for further downstream regions, as considered herein.

Figures 5 and 6 show OH and NO predictions for Flames A and B, respectively, obtained using a k-ε turbulence model to represent the mixing and velocity fields. It is noted that second-order effects are less pronounced in this instance with reference to both species at all measurement stations, although qualitatively the results display a strong degree of similitude.

Data for Flame A also show a greater level of agreement with the results obtained by Kronenburg et al. [14] who also based their predictions on an eddy-viscosity approach, which is most evident at the near-nozzle measurement station.

First-order physical space predictions of major species (5) were found to be in good agreement with experiment, and the Reynolds stress model provided superior results for NO over its k-ε counterpart [5]. Real space NO results in the present work demonstrate similar behaviour to the conditional data, but to a relatively lesser degree. The second-order results were found to generally negligibly differ with the first-order at upstream locale, and further downstream brought the predictions in line with observations across all three flames.

Conclusions

A second-order chemistry CMC has been successfully applied to three hydrogen diffusion flames of varying helium dilution. Results obtained using a k-ε turbulence closure compare favourably with those of an earlier investigation [14]. A Reynolds stress model has for the first time been implemented with second-order calculation, and observable differences in minor species predictions between the two models recorded. The variation in relative magnitude of the second-order closure between the two turbulence models is indicative of the importance played in the accuracy to which, and the method by which, the turbulence quantities are predicted.

Second-order predictions of NO would at first glance appear disappointing. However, in light of Kronenburg and Bilger's work [33], implementing differential diffusion effects on these flames, results are perhaps better than initial observations may lead to believe. The aforementioned authors report the greatest increase in NO production due to the effects at the near-nozzle locale, gradually decreasing along the length of the flame. It is hence suggested

that the present calculations, under this influence, may fall more into line with experimentally obtained data, and further work is required in this area to support this supposition.

The actions of second-order corrections upon results are observed to be greatest on the rich side of stoichiometric, being most evident in OH predictions where over-estimation is corrected in most cases. Again, the effects of differential diffusion upon the kinetics observed for lean mixtures [33] suggest that the inclusion of such will have a positive action upon agreement of results and experiment. The implication that the combined effects of differential diffusion and second-order kinetics should be investigated is once again brought to the fore.

Overall, unanswered questions remain, and in addition to the work suggested, other factors may have to be considered to explain anomalous near-nozzle NO predictions in these flames. In other applications of the same turbulence closure and CMC model by the authors, greater success in NO prediction has been achieved in CH_4 flames, leading to the suggestion that further investigation of kinetic schemes for NO pathways be undertaken. Also, the behaviour of models for scalar dissipation is highlighted for additional study. The application of Girimaji's model in the present study, although having been demonstrated to perform well [5] in these flames, may be brought under scrutiny at near-nozzle stations, and more accurate modelling may be required in these regions.

5. Nomenclature

d	- pipe diameter	^{pe}	- partial equilibrium assumption
G	- $\left\langle \Gamma''^2 \middle\vert \eta \right\rangle$	β	- beta function
k	- turbulence kinetic energy	Γ	- total number of moles
K	- Γ''^2	ε	- dissipation of k
M	- mass fraction	η	- independent sample-space variable
P	- probability density function	ρ	- density
Q	- conditional transported scalar (Γ,i,h)	χ	- scalar dissipation
u	- axial velocity	$_r$	- reaction step
w	- source term	$_i$	- reactive scalar index
W	- molecular weight	$_h$	-enthalpy
x	- axial coordinate	$_{corr}$	- corrected value
"	- fluctuation about conditional mean	$_{2or}$	- second-order corrected

6. Acknowledgements

The authors wish to express their gratitude to the EPSRC for their financial support of R.M. Woolley through a Quota award, and to Dr. A Kronenburg and Professor R.W. Bilger for valuable discussions.

7. References

1. Pope, S.B. (1985) 'PDF Methods in Turbulent Reacting Flows', *Prog. Energy Combust. Sci.*, 11: 119-192.
2. Klimenko, A.Yu. and Bilger, R.W. (1999) 'Conditional Moment Closure for Turbulent Combustion', *Prog. Energy Combust. Sci.*, 25: 595-687.
3. Smith, N.S.A., Bilger, R.W., Carter, C.D., Barlow, R.S. and Chen, J.-Y. (1995) 'A Comparison of CMC and PDF Modelling Predictions with Experimental Nitric Oxide LIF / Raman Measurements in a Turbulent H_2 Jet Flame', *Combust. Sci. Technol.*, 105: 357-375.
4. Barlow, R.S., Smith, N.S.A., Chen, J.-Y. and Bilger, R.W. (1999) 'Nitric Oxide Formation in Dilute Hydrogen Jet Flames: Isolation of the Effects of Radiation and Turbulence-Chemistry Submodels', *Combust. Flame*, 117: 4-31.
5. Fairweather, M. and Woolley, R.M. (2003) 'First-Order Conditional Moment Closure Modelling of Turbulent, Non-Premixed Hydrogen Flames', *Combust. Flame*, 133: 393-405.
6. Roomina, M.R. and Bilger, R.W. (1999) 'Conditional Moment Closure Modelling of Turbulent Methanol Jet Flames', *Combust. Theory Modelling*, 3: 689-708.
7. Roomina, M.R. (1998) 'Conditional Moment Closure Predictions for Piloted Hydrocarbon Jet Flames', *Ph.D. Thesis*, University of Sydney.
8. Smith, N.S.A. (1994) 'Development of the CMC Method for Modelling Turbulent Combustion', *Ph.D. Thesis*, University of Sydney.
9. Roomina, M.R. and Bilger, R.W. (2001) 'Conditional Moment Closure (CMC) Predictions of a Turbulent Methane-Air Jet Flame', *Combust. Flame*, 125: 1176-1195.
10. Fairweather, M. and Woolley, R.M. (2004) 'First-Order Conditional Moment Closure Modelling of Turbulent, Non-Premixed Methane Flames', *Combust. Flame*, 138: 3-19.

11. Kim, S.H., Huh, K.Y. and Tao, L. (2000) ‘Application of the Elliptic Conditional Moment Closure Model to a Two-dimensional Nonpremixed Methanol Bluff-body Flame’, *Combust. Flame*, 120: 75-90.
12. Kim, S.H. and Huh, K.Y. (2002) ‘Use of the Conditional Moment Closure Model to Predict NO Formation in a Turbulent CH_4/H_2 Flame Over a Bluff Body’, *Combust. Flame*, 130: 94-111.
13. Devaud, C.B. and Bray, K.N.C. (2003) ‘Assessment of the Applicability of Conditional Moment Closure to a Lifted Turbulent Flame: First Order Model’, *Combust. Flame*, 132: 102-114.
14. Kronenburg, A., Bilger, R.W. and Kent, J.H. (1998) ‘Second-Order Conditional Moment Closure for Turbulent Jet Diffusion Flames’, *Proc. Combust. Inst.*, 27: 1097-1104.
15. Bradley, D., Emerson, D.R., Gaskell, P.H., and Gu, X.J. (2002) ‘Mathematical Modelling of Turbulent Non-Premixed Piloted Jet Flames with Local Extinctions’, *Proc. Combust. Inst.*, 29: 2155-2162.
16. Mastorakos, E. and Bilger, R.W. (1998), ‘Second-order Conditional Moment Closure For The Autoignition of Turbulent Flows’, *Physics of Fluids*, 10: 1246-1248.
17. Kim, S.H., Huh, K.Y. and Bilger, R.W. (2002) ‘Second-Order Conditional Moment Closure Modelling of Local Extinction and Reignition in Turbulent Nonpremixed Hydrocarbon Flames’, *Proc. Combust. Inst.*, 29: 2131-2137.
18. Kim, S.H. and Huh, K.Y., (2004), ‘Second-order Conditional Moment Closure Modelling of Turbulent Piloted Jet Diffusion Flames’, *Combust. Flame*, 138: 336-352.
19. Barlow, R.S. and Carter, C.D. (1996) ‘Relationships Among Nitric Oxide, Temperature, and Mixture Fraction in Hydrogen Jet Flames’, *Combust. Flame*, 104: 288-299.
20. Jones, W.P. and Launder, B.E. (1972) ‘The Prediction of Laminarisation with a Two-Equation Turbulence Model’, *Int. J. Heat Mass Transfer*, 15: 301-314.

21. Jones, W.P. and Musonge, P. (1988) 'Closure of the Reynolds Stress and Scalar Flux Equations', *Phys. Fluids*, 31: 3589-3604.
22. el Baz, A., Craft, T.J., Ince, N.Z. and Launder, B.E. (1993) 'On the Adequacy of the Thin-shear-flow Equations for Computing Turbulent Jets in Stagnant Surroundings', *Int. J. Heat Fluid Flow*, 14 (2): 164-169.
23. Spalding, D.B. (1977) *GENMIX: A General Computer Program for Two-dimensional Parabolic Phenomena*. Pergamon Press, London.
24. Hinze, J.O. (1975), *Turbulence*, McGraw-Hill, New York.
25. Klimenko, A.Yu. (1990) 'Multicomponent Diffusion of Various Admixtures in Turbulent Flow', *Fluid Dynamics*, 25: 328-334.
26. Girimaji, S.S. (1992) **'**On the Modelling of Scalar Diffusion in Isotropic Turbulence', *Phys. Fluids*, 4: 2529-2537.
27. Kee, R.J., Rupley, F.M. and Miller, J.A. (1996) *CHEMKIN II: A FORTRAN Chemical Kinetics Package for the Analysis of Gas-Phase Chemical Kinetics*. Sandia National Laboratories, Report No. SAND89-8009B.
28. Miller, J.A. and Bowman, C.T. (1989) 'Mechanism And Modelling of Nitrogen Chemistry in Combustion', *Progress in Energy and Combustion Science*, 15: 287-338.
29. Smooke, M.D. and Giovangigli, V. (1990) 'Formulation of the Premixed and Nonpremixed Test Problems', in M.D. Smooke, (ed.), *Reduced Kinetic Mechanisms and Asymptotic Approximations For Methane-Air Flames, Lecture Notes in Physics 384*, 1-28, Springer-Verlag, Berlin.
30. Li, J.D. and Bilger, R.W. (1993) 'Measurement and Prediction of the Conditional Variance in a Turbulent Reactive-Scalar Mixing Layer', *Phys. Fluids*, 5: 3255-3264.

31. Chen, J.-Y. (1988) ‘A General Procedure For Constructing Reduced Reaction Mechanisms With Given Independent Relations’, *Combustion Science And Technology*, 57: 89-94.
32. Montgomery, C.J., Kosály, G. and Riley, J.J. (1997) ‘Direct Numerical Simulation of Turbulent Nonpremixed Combustion with Multistep Hydrogen-Oxygen Kinetics’, *Combust. Flame*, 109: 113-144.
33. Kronenburg, A. and Bilger, R.W. (2001) ‘Modelling Differential Diffusion in Nonpremixed Reacting Turbulent Flow: Application to Turbulent Jet Flames’, *Combust. Sci. Technol.*, 166: 175-194.

8. Tables

Reaction	A	b	E
O2 + H = OH + O	2.00E+14	0	16800
OH + O = H + O2	1.57E+13	0	841.3
H2 + O = OH + H	5.06E+04	2.67	6286
H + OH = O + H2	2.22E+04	2.67	4371
H2 + OH = H2O + H	1.00E+08	1.6	3298
H2O + H = H2 + OH	4.31E+08	1.6	18274
O + H2O = OH + OH	1.47E+10	1.14	16991
OH + OH = H2O + O	1.59E+09	1.14	100.4
H + O2 + M = HO2 + M	2.30E+18	-0.8	0
H + HO2 = OH + OH	1.50E+14	0	1004
H + HO2 = H2 + O2	2.50E+13	0	693.1
H + HO2 = H2O + O	3.00E+13	0	1721
OH + HO2 = H2O + O2	6.00E+13	0	0
O + HO2 = OH + O2	1.80E+13	0	-406.3
HO2 + HO2 = H2O2 + O2	2.00E+12	0	0
HO2 + H2O = H2O2 + OH	2.86E+13	0	32790
H2O2 + OH = HO2 + H2O	1.00E+13	0	1800
H2O2 + M = OH + OH + M	1.30E+17	0	45500
OH + OH + M = H2O2 + M	9.86E+14	0	-5070
OH + H + M = H2O + M	2.20E+22	-2	0
H + H + M = H2 + M	1.80E+18	-1	0
O + N2 = NO + N	1.40E+14	0	75800
N + O2 = NO + O	6.40E+09	1	6280
OH + N = NO + H	4.00E+13	0	0
NO + HO2 = NO2 + OH	2.11E+12	0	-480
NO2 + H = NO + OH	3.50E+14	0	1500

Table 1 – Hydrogen/Air Combustion Mechanism Scheme
(Units: mole, m^3, s, K, cal)

9. Figure Captions

Figure 1. Calculated conditional velocity and scalar dissipation at three axial locations in Flame A (— predicted Re-stress, -·- predicted k-ε).

Figure 2. Measured and predicted major species and temperatures in Flame A, obtained using the Reynolds stress turbulence model (o measured, — 1st order CMC, -·- 2nd order CMC).

Figure 3. Measured and predicted OH and NO mass fractions in Flame A, obtained using the Reynolds stress turbulence model (o measured, — 1st order CMC, -·- 2nd order CMC).

Figure 4. Measured and predicted OH and NO mass fractions in Flame B, obtained using the Reynolds stress turbulence model (o measured, — 1st order CMC, -·- 2nd order CMC).

Figure 5. Measured and predicted OH and NO mass fractions in Flame A, obtained using the k-ε turbulence model (o measured, — 1st order CMC, -·- 2nd order CMC).

Figure 6. Measured and predicted OH and NO mass fractions in Flame B, obtained using the k-ε turbulence model (o measured, — 1st order CMC, -·- 2nd order CMC).

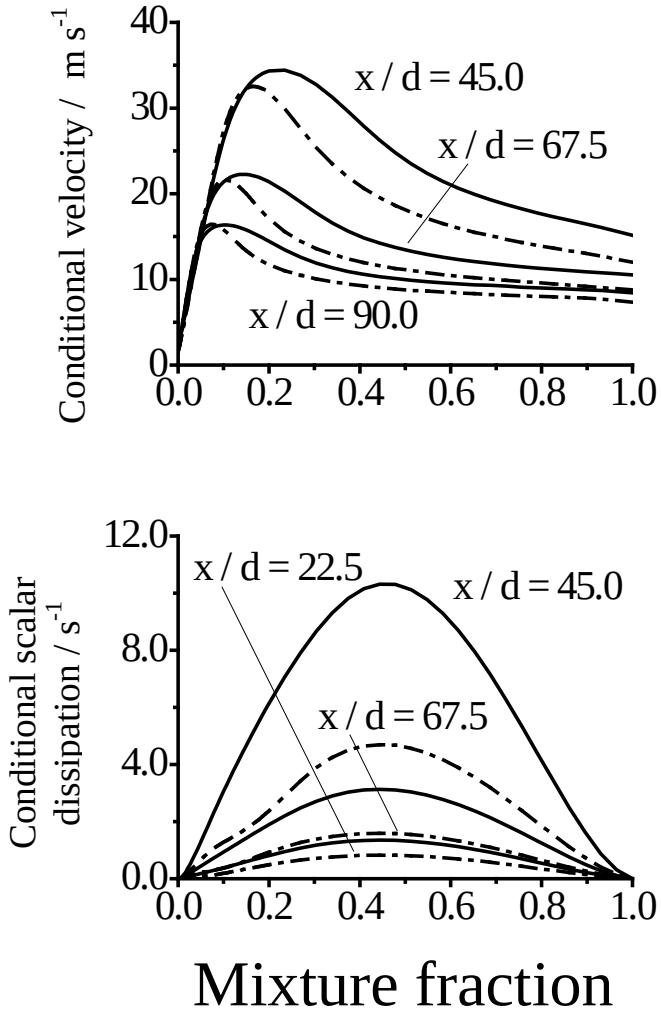
Conditional velocity / m s-1
40
30
20
10
0
0.0
0.2
0.4
0.6
0.8
1.0
x / d = 45.0
x / d = 67.5
x / d = 90.0
Conditional scalar dissipation / s-1
12.0
8.0
4.0
0.0
x / d = 22.5
x / d = 45.0
x / d = 67.5
Mixture fraction

Fig. 1

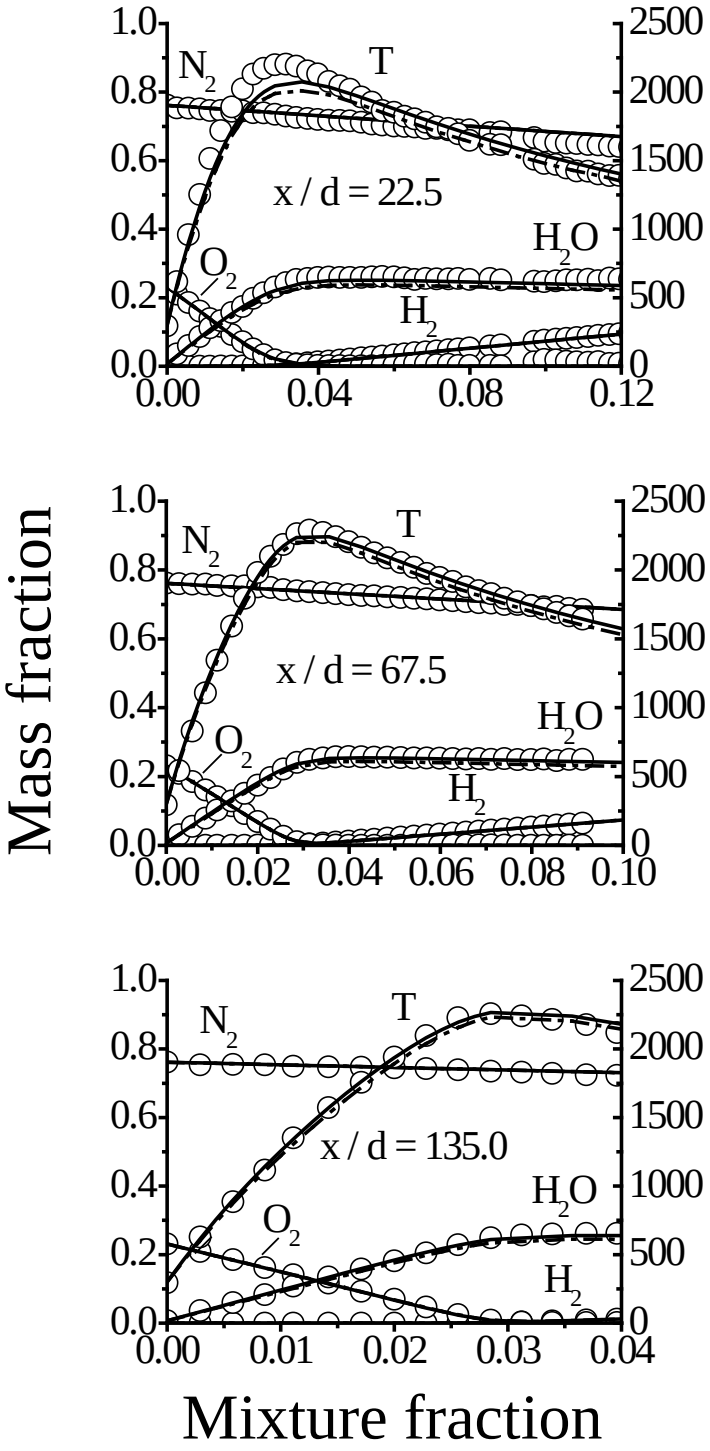
Mass fraction
1.0
0.8
0.6
0.4
0.2
0.0
2500
2000
1500
1000
500
0
N2
T
x / d = 22.5
H2O
O2
H2
0.00
0.04
0.08
0.12
x / d = 67.5
0.02
0.06
0.10
x / d = 135.0
0.01
0.03
Mixture fraction

Fig. 2

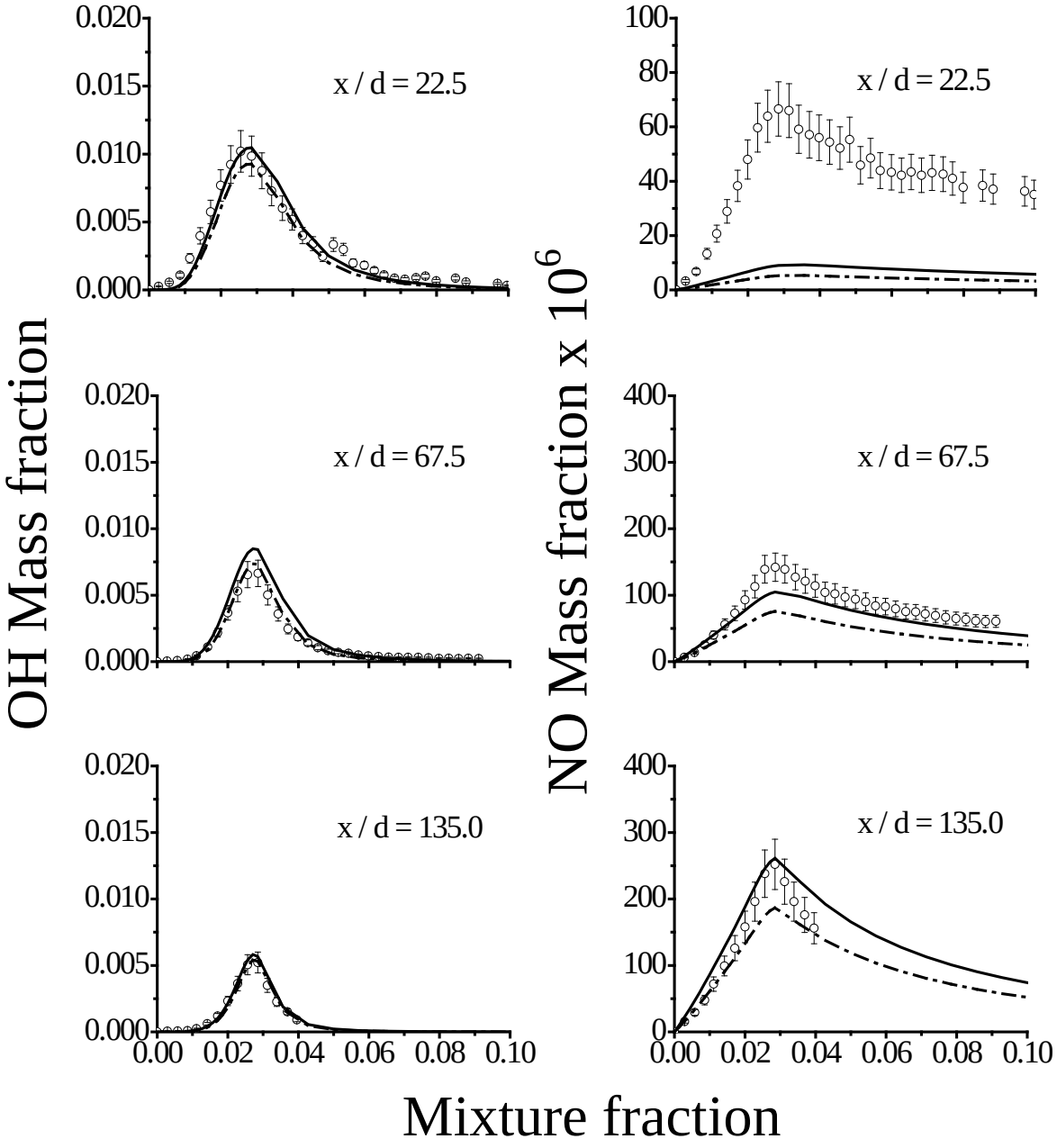
OH Mass fraction
NO Mass fraction x 10^6
Mixture fraction
x / d = 22.5
x / d = 67.5
x / d = 135.0
0.020
0.015
0.010
0.005
0.000
100
80
60
40
20
0
400
300
200
100
0.00
0.02
0.04
0.06
0.08
0.10

Fig. 3

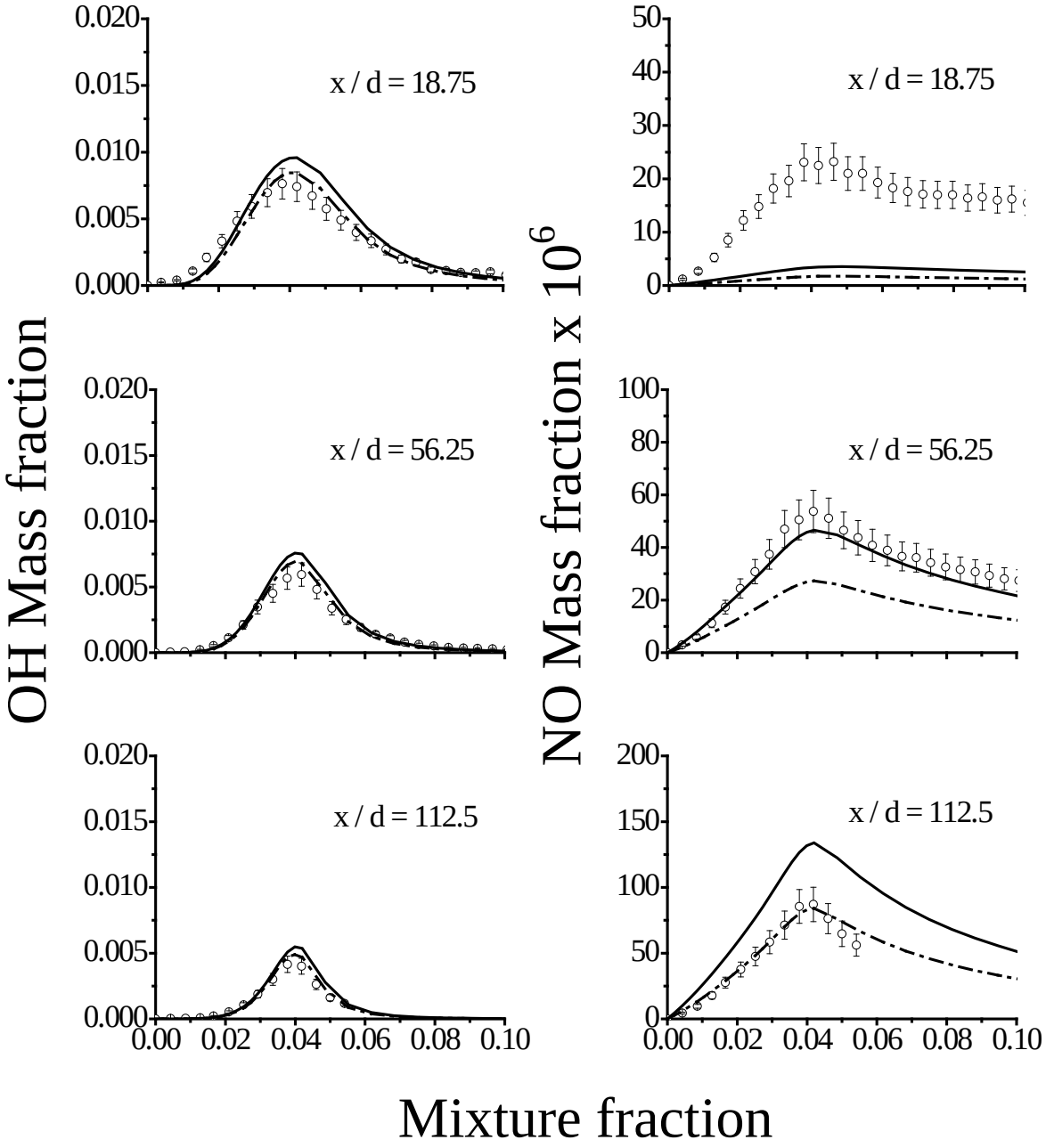
OH Mass fraction
NO Mass fraction x 10^6
x / d = 18.75
x / d = 56.25
x / d = 112.5
0.020
0.015
0.010
0.005
0.000
50
40
30
20
10
0
100
80
60
40
20
200
150
100
50
0.00
0.02
0.04
0.06
0.08
0.10
Mixture fraction

Fig. 4

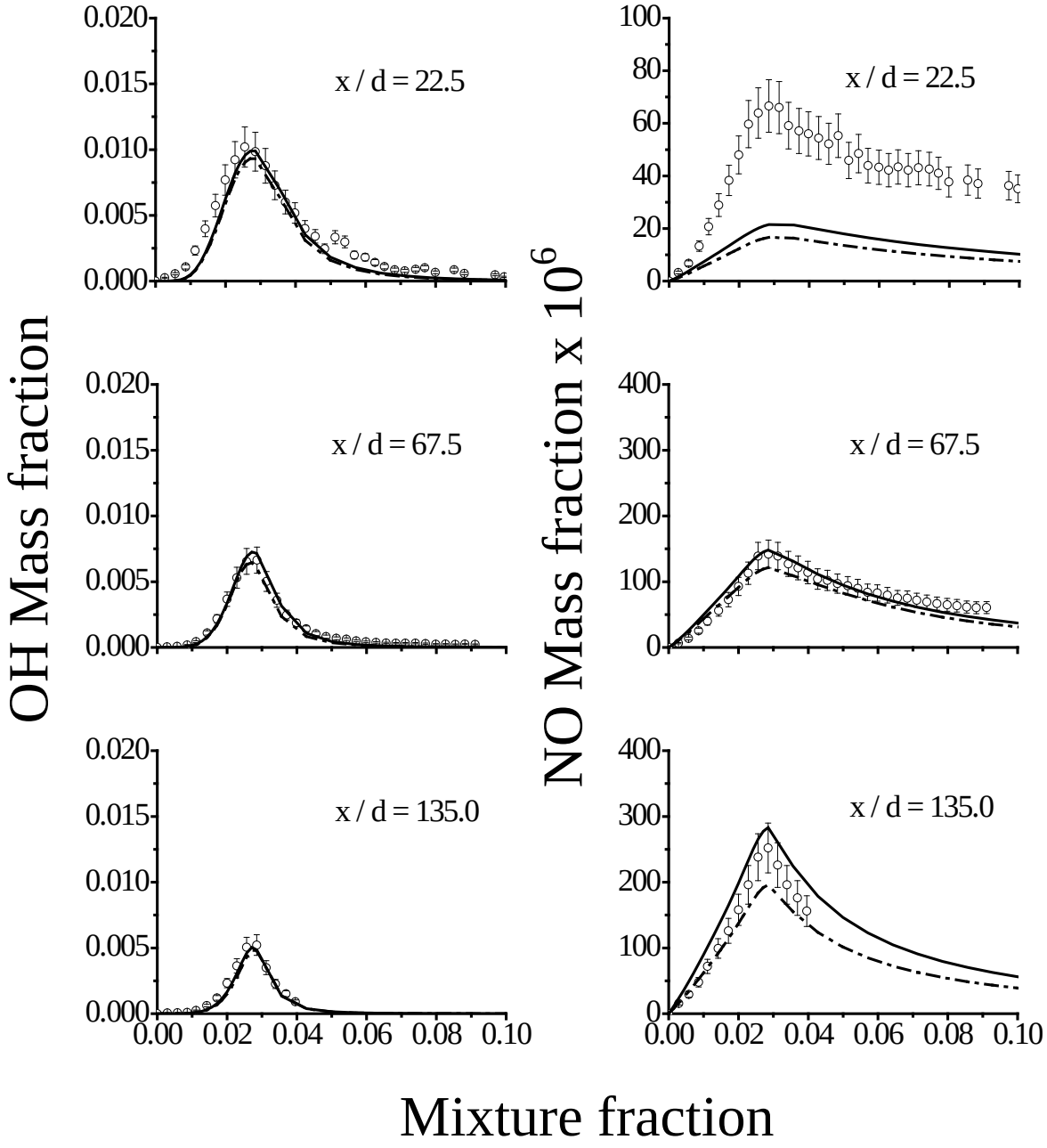
OH Mass fraction
NO Mass fraction x 10^6
x / d = 22.5
x / d = 67.5
x / d = 135.0
0.020
0.015
0.010
0.005
0.000
100
80
60
40
20
0
400
300
200
100
0.00
0.02
0.04
0.06
0.08
0.10
Mixture fraction

Fig. 5

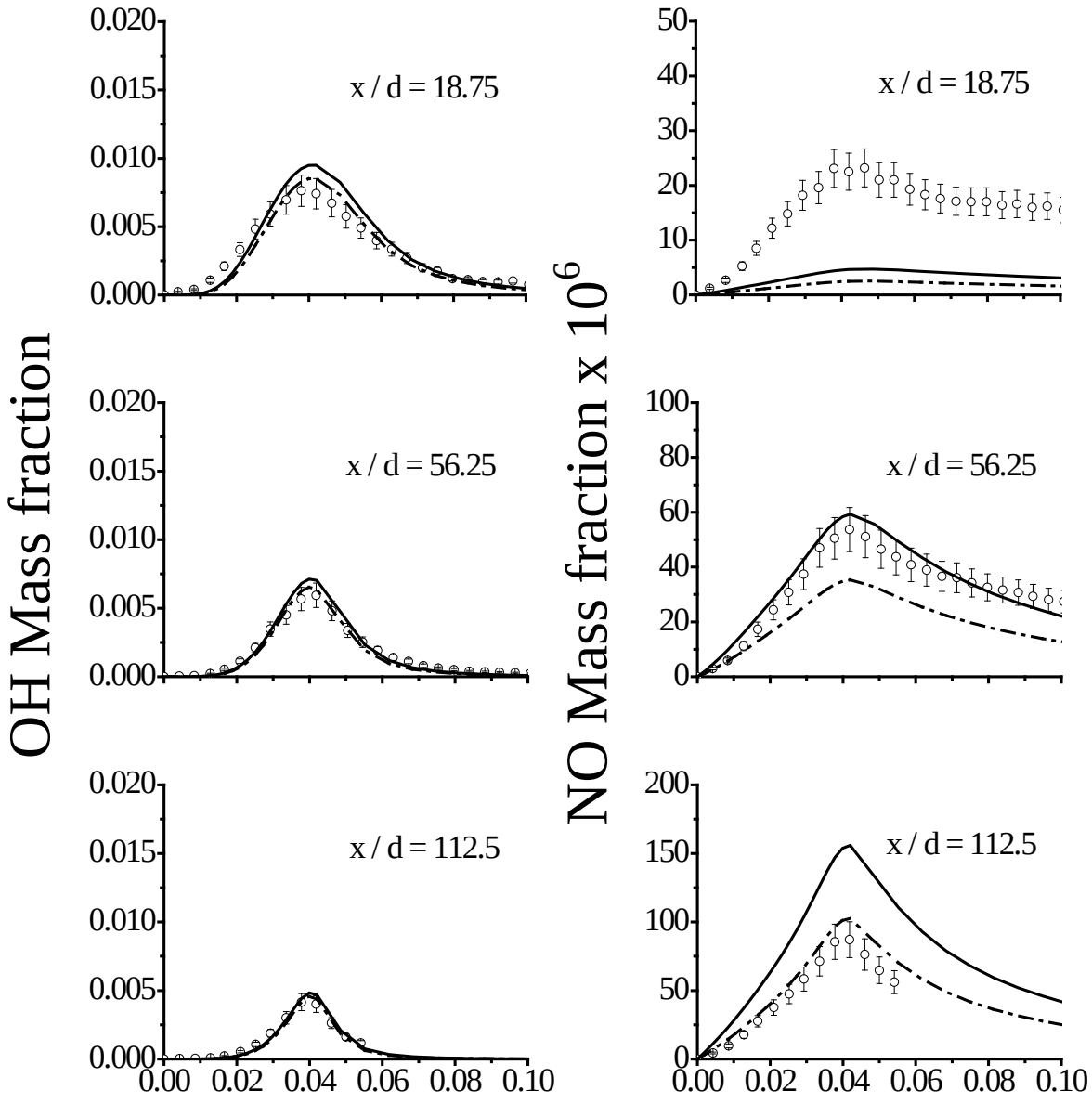
OH Mass fraction
NO Mass fraction x 10^6
x / d = 18.75
x / d = 56.25
x / d = 112.5
0.020
0.015
0.010
0.005
0.000
50
40
30
20
10
0
100
80
60
40
20
200
150
100
50
0.00
0.02
0.04
0.06
0.08
0.10
Mixture fraction

Fig. 6